

Mass Analyzed Threshold Ionization Spectroscopy of *o*-, *m*-, and *p*-Dichlorobenzenes. Influence of the Chlorine Position on Vibrational Spectra and Ionization Energy

Angela Gaber, Mikko Riese, and Juergen Grotemeyer*

Institute for Physical Chemistry, Christian Albrechts University Kiel, Ludewig-Meyn-Strasse 8, 24118 Kiel, Federal Republic of Germany

Received: June 20, 2007; In Final Form: October 16, 2007

For the first time, vibrational spectra of the $^{35}\text{Cl}_2$ and $^{35}\text{Cl}^{37}\text{Cl}$ isotopomers of *o*-, *m*-, and *p*-dichlorobenzene cations in the electronic ground state have been measured via S_1 intermediate states by mass analyzed threshold ionization (MATI) spectroscopy. Additionally, ab initio calculations at DFT (density functional theory), CIS (configuration interaction singles), and CASSCF (complete active space self-consistent field) levels of theory have been conducted to compare experimental findings with theory. From the MATI spectra, adiabatic ionization energies of the ortho, meta, and para isomers have been determined to be the same for each pair of investigated isotopomers to $73\,237 \pm 6$, $72\,191 \pm 6$, and $73\,776 \pm 6 \text{ cm}^{-1}$, respectively. Several vibrational modes, including fundamentals, combinations, and progressions have been assigned by comparing the experimental and theoretical results. The appearance of overtone progressions involving the 7a mode could be explained by a geometry change of all three isomers during ionization in the direction of this mode by retraining the symmetry of the molecules. Although the general spectral features of the investigated isotopomers are similar, frequencies of some vibrations are slightly different up to a few wavenumbers depending on the involvement of the chlorine atoms in the molecular motion.

Introduction

Chlorinated aromatic molecules are a topic of great interest because of their widespread presence and their potential toxic and/or carcinogenic properties. Chlorobenzene has been subject of several investigations studying the first excited state as well as the cation ground state.^{1–3}

The substitution of two hydrogen atoms of the aromatic ring by other substituents can change the electron distribution in the molecule. This can cause changes in the transition energies, ionization energy, and the molecular geometry, the latter seen by alterations in the vibrations in the excited electronic state and the ground ionic state. The magnitude of these effects depends on the relative position of the two substituents. The influence of the relative positions of the substituents on the excitation energy and the ionization energy was investigated for the constitutional isomers of difluorobenzene, fluorophenol, and the fluoroaniline.^{4–12} In this paper we extend the measurements to the dichlorobenzenes to examine if the same trends were observed for these constitutional isomers, especially for the ionization energies.

As the changes are mostly small (from a few wavenumbers (cm^{-1}) up to a few hundreds of wavenumbers), the investigations require powerful, high-resolution examination methods, such as mass analyzed threshold ionization (MATI) or zero-kinetic energy (ZEKE) spectroscopy.^{7,13,14} The former has the advantage of mass separation and therefore offers great possibilities for the investigation of two or more isotopomers.

Investigations on dichlorobenzene isomers have rarely been performed. The first excited states have been the subject of a couple of investigations. First, Anno et al.¹⁵ recorded near-ultraviolet absorption spectra of *o*-dichlorobenzene (*o*DCB) and

p-dichlorobenzene (*p*DCB). Shimoda et al.¹⁶ obtained the fluorescence lifetimes of dichlorobenzene molecules in the S_1 state and assigned some of the fundamental vibrations. Furthermore, Weickardt et al.¹⁷ showed a possible differentiation of the three isomers with resonance-enhanced multiphoton ionization (REMPI) spectroscopy as the transition energies as well as the vibrations differ strongly from each other. Finally, Rohlfing et al.¹⁸ as well as Sands and co-workers¹⁹ assigned the vibrational modes in the first excited state of *p*DCB. For the ortho and meta isomers a detailed assignment has yet not been published.

For the ionic ground state the performed examinations are rare. Vibrationally resolved spectra of matrix isolated *p*DCB ion have been performed by Szczepanski et al.,²⁰ but vibrationally resolved spectra of the ionic ground state in the gas phase are still missing for all three dichlorobenzenes.

In the following we report on theoretical calculations and MATI measurements via vibronic states of the three dichlorobenzenes.

Experimental Setup

The experimental setup consists of a home-built time-of-flight mass spectrometer as described in detail elsewhere.^{21,22} Therefore, only a brief description is given here.

The spectrometer consists of a standard second order corrected reflectron time-of-flight mass spectrometer and a single-stage ion source. The dichlorobenzene isomers were purchased from Sigma-Aldrich and used without further purification. A supersonic beam is produced by expanding the sample seeded in argon with a backing pressure of 2 bar through the orifice of a pulsed valve. After skimming, the jet enters the ion source where the multiphoton absorption takes place. Two different dye lasers pumped with the same Nd:YAG laser are used for exciting and

* Corresponding author. Telephone: (049) 431 880 2843. Fax: (049) 431 880 2848. E-mail: grote@phc.uni-kiel.de.

ionizing the molecules. This experimental setup guarantees a very low jitter and therefore a stable signal-to-noise ratio. The output of each dye laser was frequency doubled by a BBO-I crystal yielding tunable ranges from 260 to 280 nm. Wavelength calibration of both dye lasers was performed by recording an optical galvanic spectrum with a neon hollow cathode lamp yielding accuracy better than 2 cm^{-1} .

The excitation of the molecules by the incident lasers is performed in all experiments under field-free conditions. To observe the MATI spectra, a small electric field of $1\text{--}2\text{ V/cm}$ is applied after 100 ns to separate any prompt ions from the Rydberg molecules. After $5\text{ }\mu\text{s}$ the Rydberg neutrals are field ionized by switching on an electric field (890 V/cm) through a Behlke HS56-01 fast transistor. The formed ions are accelerated into the mass spectrometer. The mass-separated ions are detected by a conventional dual-plate detector. The detector signal is measured and visualized by a LeCroy 534M digital oscilloscope and transferred to a computer for further investigations.

Results from Theoretical Calculations

To support the experimental findings and to assign the observed vibrational structures, quantum chemical calculations have been performed using the Gaussian 03 software package.²³

1. Geometry and Frequency Calculations. Geometry optimizations and harmonic frequencies for the optimized molecular structures of the neutral and cation ground states have been calculated using the density functional theory (DFT) at the Becke 3LYP functional²⁴ level with the basis set 6-311++G(d,p). For the neutral ground state the calculated frequencies obtained with the DFT method fit very well with the experimental results from Scheerer et al.²⁵ for all three isomers. This was a hint that the used basis set and the resulting molecular geometry may serve as a reference for the calculations of the first excited state and the ion ground state.

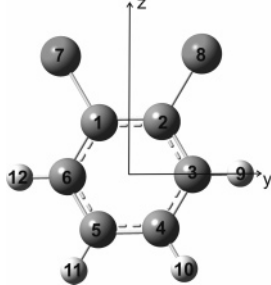
For good agreement between the experimental and the theoretical results, scaling factors for the calculated frequencies of the S_1 state of 0.95 and for the cation state frequencies of 0.98 were used.

For the assignment of the vibrations we followed Wilson nomenclature,²⁶ and the numbering convention used for normal vibrations follows Lord's scheme.²⁷ Further on, also the Herzberg nomenclature²⁸ (frequently called the Mulliken notation²⁹) is given in parentheses in the tables.

For the first excited state, calculations at the CIS level³⁰ and at the CASSCF level were performed with the same basis set. For the CASSCF calculations an active space consisting of six π orbitals containing six electrons was chosen involving the three highest occupied π orbitals (HOMOs) of the aromatic ring and the three lowest unoccupied π^* orbitals (LUMOs). We assume for the electronic excitation a $\pi^* \leftarrow \pi$ transition without any involvement of the lone-pair electrons of the chlorine atoms. From UV photoelectron spectra it is known that the lone-pair orbitals of the chlorine lie 1.5 eV under the aromatic π orbitals.³¹ Therefore, they contribute only very weakly to the electronic excitation. As shown in Tables 1–3, the electronic excitation causes an extension of the aromatic ring in the three isomers due to a weakening of the π bond. This corresponds to a $\pi^* \leftarrow \pi$ excitation. Simultaneously, a reduction of the C–Cl bond is observed as the chlorine atoms stabilize the ring by the mesomeric effect. We observe no characteristic differences between the isomers.

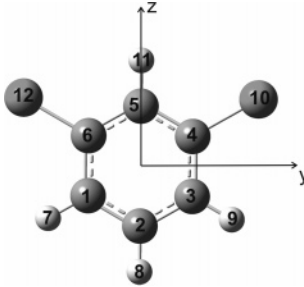
In the cation state the NBO analysis of the *o*DCB cation shows that the positive charge is primarily located in a π^* orbital spanning the C3–C4–C5–C6 atoms (see Table 1); thus the

TABLE 1: Geometries of *o*DCB Calculated at the DFT Level and the 6-311++G(d,p) Basis Set for the S_0 and D_0 States and at the CIS/6-311++G(d,p) Level for the S_1 State



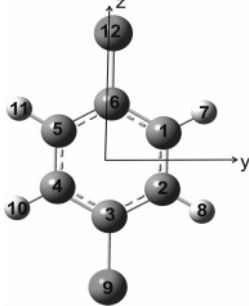
	S_0	S_1	D_0
C1–C2	1.3982	1.4179	1.4607
C2–C3	1.3944	1.4118	1.4009
C3–C4	1.3906	1.4097	1.3785
C4–C5	1.3935	1.4095	1.4306
C1–Cl7	1.7480	1.7135	1.6922
C3–H9	1.0825	1.0712	1.0823
C4–H10	1.0834	1.0732	1.0837
C1–C2–C3	119.794	120.204	119.685
C2–C3–C4	120.210	119.344	119.372
C3–C4–C5	119.995	120.452	120.943
C1–C2–Cl8	121.454	121.493	120.516
C2–C3–H9	118.952	119.407	119.301
C3–C4–H10	119.556	119.557	119.812

TABLE 2: Geometries of *m*DCB Calculated at the DFT Level and the 6-311++G(d,p) Basis Set for the S_0 and D_0 States and at the CIS/6-311++G(d,p) Level for the S_1 State



	S_0	S_1	D_0
C1–C2	1.3930	1.4109	1.3876
C1–C6	1.3913	1.4090	1.4407
C6–C5	1.3917	1.4099	1.3895
C1–H7	1.0819	1.0721	1.0835
C2–H8	1.0837	1.0720	1.0827
C6–Cl12	1.7567	1.7189	1.7014
C5–H11	1.0810	1.0701	1.0817
C1–C2–C3	120.975	119.642	119.416
C2–C1–C6	118.753	119.520	119.919
C1–C6–C5	121.685	122.058	121.554
C4–C5–C6	118.148	117.202	117.639
C1–C2–H8	119.513	120.179	120.292
C2–C1–H7	121.051	120.902	121.281
C5–C6–Cl12	118.858	118.800	120.537
C6–C5–H11	120.926	121.399	121.181

C-atoms are not neighbors of the two chlorine atoms. The calculated geometry shows a further decrease of the C–Cl bond length, together with an elongation of the C1–C2 bond and a compression of the C3–C4 bond. For the *m*DCB cation the aromatic ring is stretched along the z -axis (Table 2). The C1–C6 bond length is dramatically increased to 1.441 \AA , whereas the C–Cl bond length is reduced, but less than for the other two isomers. This indicates a weaker stabilization by the chlorine atoms by the mesomeric effect. For the para isomer, after

TABLE 3: Geometries of *p*DCB Calculated at the DFT Level and the 6-311++G(d,p) Basis Set for the S_0 and D_0 States and at the CIS/6-311++G(d,p) Level for the S_1 State


	S_0	S_1	D_0
C1–C2	1.3928	1.4102	1.3660
C2–C3	1.3914	1.4093	1.4248
C1–H7	1.0824	1.0712	1.0732
C3–Cl9	1.7569	1.7160	1.6857
C1–C2–C3	119.48	118.66	119.40
C2–C3–C4	121.05	122.67	121.21
H7–C1–C2	120.23	121.18	121.33
Cl9–C3–C2	119.48	118.66	119.40

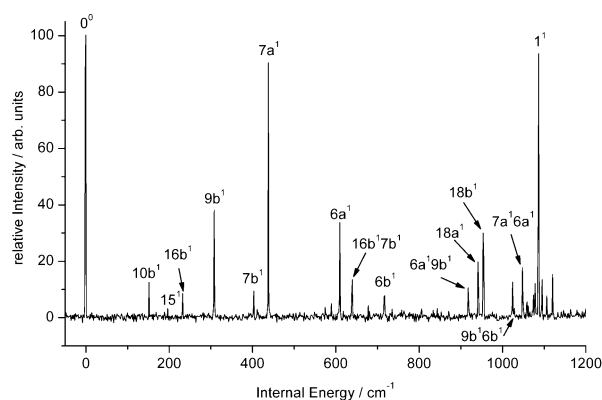
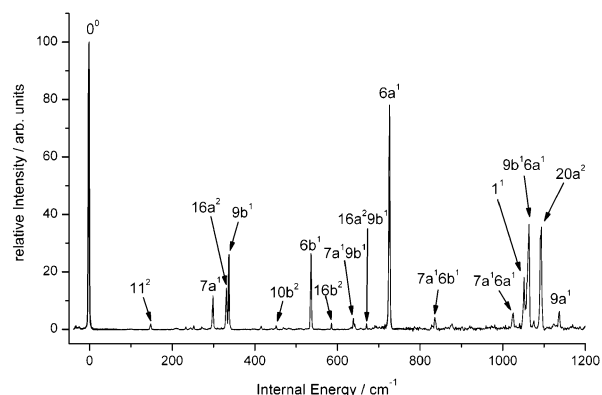
removal of an electron of the π^* orbital, the aromatic ring is stretched along the z -axis as well (Table 3). Thus the C2–C3 bond becomes weaker, whereas the C1–C2 bond is strongly reduced to 1.366 Å and the C–Cl bond to 1.687 Å, respectively.

For *o*DCB and *p*DCB the geometry changes result in a more quinoid structure of the cations. In the case of the *m*DCB cation a quinoid structure is not possible. The positive charge cannot be stabilized to the same amount, which results in a higher ionization energy than for the two other isomers. However, in all three isomers the C–Cl bond and the central C–C bond are shortened. These changes in the structure are consistent with an electron being removed from a π orbital of the benzene ring and the positive charge being partially quenched by donation of a lone-pair electron of the chlorine atoms (mesomeric effect).

Kwon et al.³² introduced a method to calculate the overlap of the eigenvector of the excited mode and the geometry change during excitation. Therefore, the atomic displacement vector during excitation is mass-weighted and its projection on the eigenvector of the modes is calculated. With this an exact value for the concordance between geometry changes and eigenvectors of the mode involved could be computed. For the total symmetric modes of the ortho isomer for the ionization from the excited state the greatest values are given for 15^1 (0.46), $7a^1$ (0.47), and $6a$ (0.13). In the case of the meta isomer the absolute values for the overlap were calculated to be 0.37 for the $9a^1$ mode, 0.63 for the $7a^1$, and 0.10 for the $6a^1$. Last, for the para isomer, the absolute values for the overlap are given by 0.77 for the $7a^1$ mode, 0.08 for the $6a^1$, and 0.08 for the 1^1 .

2. Energy Calculations. With the results of the CASSCF calculations we were able to estimate the electronic transition energies to the first excited state for the investigated ortho, meta, and para isomers to be $37\,122\text{ cm}^{-1}$ (4.6026 eV), $37\,259\text{ cm}^{-1}$ (4.6196 eV), and $37\,039\text{ cm}^{-1}$ (4.5923 eV), respectively. The calculated values for the ionization energy at the DFT level are 9.0803, 8.728, and 8.916 eV, respectively.

Additionally, the symmetries and energies of higher electronically excited states for the neutral molecule were calculated at the time-dependent density functional theory (TD-DFT) level with the basis set 6-311++G(d,p) in order to explain the appearance of vibrations in the REMPI spectra which are allowed by vibronic coupling to higher electronic states.

**Figure 1.** $(1 + 1')$ REMPI spectrum of *o*DCB in the first electronically excited state. The electronic origin of the S_1 state is determined to $36\,217\text{ cm}^{-1}$.**Figure 2.** $(1 + 1')$ REMPI excitation spectrum of the first excited state of *m*DCB. The electronic origin of the S_1 state is determined to $36\,193\text{ cm}^{-1}$.

Experimental Results

In accordance with the natural abundance of chlorine, the time-of-flight mass spectra show a pattern of three peaks from the $^{35}\text{Cl}_2$, $^{35}\text{Cl}^{37}\text{Cl}$, and $^{37}\text{Cl}_2$ isotopomers of dichlorobenzene. The theoretical ratio of the intensity of the masses 146:148:150 is 9.3:6.1:1.0. As the mass signal of the heaviest isotopomer is only very weakly observed, we only recorded the two main isotopomers.

In the following we will give the frequency shift between the isotopomers in square brackets after the frequency of the $^{35}\text{Cl}_2$ isotopomer.

1. REMPI Spectra of the First Excited State. For the identification of the vibrational levels of the S_1 state which are used as intermediate states for the MATI spectroscopy, $(1 + 1')$ REMPI spectra of the first electronically excited state as shown in Figures 1–3 were recorded. To obtain these spectra, the wavelength of the first laser was tuned from 265 to 280 nm while the second laser was kept constant at 260 nm for ionizing the molecules.

For all three isomers the calculated frequencies for the $^{35}\text{Cl}_2$ isotopomers in the first excited state at the CASSCF level as well as the calculated shifts from the $^{35}\text{Cl}^{37}\text{Cl}$ isotopomers are listed in Table 4. Also, the calculated frequencies for the ion ground state are given here. In Tables 5–7 all observed vibrations for the three isomers in the first excited state are listed.

(a) *o*DCB. *o*DCB belongs to the point group C_{2v} . The $S_1 \leftarrow S_0$ transition corresponds to a ${}^1A_1 \leftarrow {}^1A_1$ excitation. The origin of the first electronically excited state was observed for the $^{35}\text{Cl}_2$ and the $^{35}\text{Cl}^{37}\text{Cl}$ isotopomers at $36\,238 \pm 3\text{ cm}^{-1}$. This value accords well with the results obtained by Anno et al.¹⁵ They

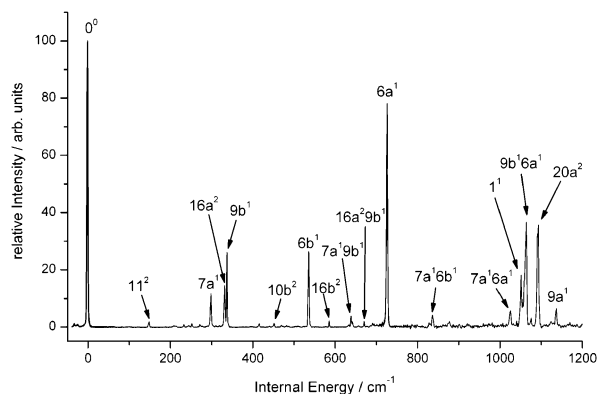


Figure 3. $(1 + 1')$ REMPI excitation spectrum of the first excited state of *p*DCB. The electronic origin of the S_1 state is determined to $35\,752\text{ cm}^{-1}$.

measured by near-ultraviolet absorption spectroscopy the electronic origin at about $36\,232\text{ cm}^{-1}$. Shimoda et al.¹⁶ found a value of 275.9 nm ($36\,245\text{ cm}^{-1}$) by recording fluorescence spectra of *o*DCB. While these results are close to our measured value, the two-color REMPI spectrum obtained by Weickardt et al.¹⁷ results for the $0-0$ transition in a value of 276.11 nm corresponding to $36\,217\text{ cm}^{-1}$. The deviation from our result seems to be based on the use of vacuum wavelength for laser calibration, whereas in our work air wavelength was used.

Assignment of the Vibrations. a_1 Symmetry: Shimoda et al.¹⁶ assigned the peaks appearing at 610 cm^{-1} [1.4 cm^{-1}] and 1088 cm^{-1} [1.2 cm^{-1}] as the vibrations $6a^1$ and 1^1 , respectively. For these vibrations the assignment is kept because the measured frequencies are in good accordance with the calculated ones of 602 cm^{-1} [1.3 cm^{-1}] and 1069 cm^{-1} [0.7 cm^{-1}].

Two further bands at 197 cm^{-1} [2.2 cm^{-1}] and 954 cm^{-1} [0.0 cm^{-1}] were identified as a_1 vibrations by Anno and Matubara.¹⁵ We assigned these as the 15^1 and $18b^1$ vibrations, for which the calculated frequencies are given by 195 cm^{-1} [2.8 cm^{-1}] and 915 cm^{-1} [0.1 cm^{-1}]. Further on, they assigned the band at 437 cm^{-1} [2.4 cm^{-1}] as a vibration with b_1 symmetry because it was only observed with low intensity. In the spectrum presented here the intensity is indeed very high, indicating that the symmetry of the vibration is a_1 . Besides, the highest calculated shift for vibrations with b_1 symmetry is 0.2 cm^{-1} , which differs strongly from the experimentally obtained value. The calculated and measured frequencies and shifts match best when assigning this vibration as $7a^1$ mode, as the calculated frequency of the $7a^1$ mode is 444 cm^{-1} [2.4 cm^{-1}].

b_1 Symmetry: Anno et al.¹⁵ also detected the two bands appearing at 149 cm^{-1} [0.0 cm^{-1}] and 233 cm^{-1} [0.0 cm^{-1}], but no assignment was given by them. The assignment of the vibrations with $10b^1$ and $16b^1$ holds the best conformity between experiment and calculation which yields the values of 148 cm^{-1} [0.1 cm^{-1}] and 277 cm^{-1} [0.2 cm^{-1}]. Another possible assignment for the peak at 149 cm^{-1} would be $10a^2$. Swinn and Kable³³ observed such a transition in *o*-difluorobenzene with the same intensity as in the spectrum presented here. But as the calculated shift for this mode is 0.8 cm^{-1} , we keep the assignment of $10b^1$.

b_2 Symmetry: The peaks at 309 cm^{-1} [2.7 cm^{-1}], 404 cm^{-1} [1.3 cm^{-1}], and 718 cm^{-1} [1.4 cm^{-1}] show great isotopic shifts. Comparing these values with the calculated shifts, the vibrations must be assigned as $9b^1$, $7b^1$, and $6b^1$. The assignment for the $9b^1$ vibration is also supported from the measurement performed by Anno et al.,¹⁵ who assigned the peak at 309 cm^{-1} as a band with b_2 or a_2 symmetry.

The appearance of symmetry-forbidden vibration with b_1 and b_2 symmetries may be explained due to vibronic coupling to higher excited states. These states must have B_1 and B_2 symmetries, respectively. The performed calculations at the TD-SCF level predict such states to lie 0.52 and 0.60 eV above the first excited state. The same kind of coupling was observed for *o*-difluorobenzene³⁴ and explained by a benzene-like Herzberg–Teller (HT) coupling.

(b) *m*DCB. *m*DCB belongs as well to the point group C_{2v} . The electronic excitation into the S_1 state is a ${}^1B_2(S_1) \leftarrow {}^1A_1(S_0)$ transition. Even though *m*DCB and *o*DCB both have C_{2v} symmetry, their first electronically excited states have different symmetries as the axis of highest symmetry, the z -axis, is placed through the carbon atoms in the case of *m*DCB and through the C–C bonds in the *o*DCB case. Nevertheless, the nodal properties of these states with respect to the aromatic ring are the same.

The origin of the first excited state is observed at $36\,193 \pm 3\text{ cm}^{-1}$ ($4.4874 \pm 0.0004\text{ eV}$), which is in perfect agreement with the results of Shimoda¹⁶ of $36\,193\text{ cm}^{-1}$. The deviation from the results obtained by Weickardt et al.¹⁷ of $36\,174\text{ cm}^{-1}$ can again be explained by the use of vacuum wavelength for laser calibration in their work.

Assignment of Vibrations. a_1 Symmetry: For the peaks appearing at 961 cm^{-1} [0.0 cm^{-1}] and 1103 cm^{-1} [0.6 cm^{-1}], we keep the assignment from Shimoda et al.¹⁶ with 12^1 and 1^1 , as the calculated frequencies for these vibrations are 961 cm^{-1} [0.0 cm^{-1}] and 1114 cm^{-1} [0.6 cm^{-1}].

Meenakshi and Ghosh³⁵ determined the symmetry of the peaks appearing at 365 cm^{-1} [3.3 cm^{-1}] and 607 cm^{-1} [1.1 cm^{-1}] to be a_1 , and we assigned them as the $7a^1$ and $6a^1$ vibrations. Frequency calculations for these vibrations result in 379 cm^{-1} [3.8 cm^{-1}] and 623 cm^{-1} [1.0 cm^{-1}].

For two peaks at 201 cm^{-1} [1.3 cm^{-1}] and 1090 cm^{-1} [0.0 cm^{-1}], no assignment has been given until now. We assign them as $9a^1$ and $18a^1$ due to comparison with the theoretical results.

b_2 Symmetry: Shimoda et al.¹⁶ assigned the peak at 378 cm^{-1} [1.9 cm^{-1}] as the $7a^1$ mode with a_1 symmetry. Because we already assigned the peak at 365 cm^{-1} as the $7a$ vibration and the calculated shift for the $7a^1$ mode is twice the measured one for the peak at 378 cm^{-1} , we reassigned this vibration as the 15^1 mode having b_2 symmetry. Here the calculations deliver a frequency of 360 cm^{-1} [1.8 cm^{-1}]. This assignment is consistent with the results from Meenakshi and Ghosh,³⁵ who assigned this as a vibration with b_2 symmetry.

We assign the peaks at 390 cm^{-1} [0.6 cm^{-1}] and 762 cm^{-1} [0.8 cm^{-1}] as $7b^1$ and $6b^1$, because the frequencies are in good accordance with the calculated ones of 398 cm^{-1} [1.6 cm^{-1}] and 764 cm^{-1} [1.8 cm^{-1}].

a_2 Symmetry: The peak at 680 cm^{-1} [0.0 cm^{-1}] is assigned as the $16a^2$ vibration, which is in accordance with the results from Meenakshi and Ghosh,³⁵ resulting in a frequency of 340 cm^{-1} for the $16a^1$ vibration. The peak at 270 cm^{-1} [0.3 cm^{-1}] is assigned as $10a^2$ as the calculated frequency for this overtone vibration is 278 cm^{-1} [0.6 cm^{-1}], so the frequency of the fundamental vibration $10a^1$ results in 135 cm^{-1} .

b_1 Symmetry: A peak appearing at 504 cm^{-1} [0.0 cm^{-1}] is assigned as the $16b^2$ vibration, which is in accordance with the results from Meenakshi and Ghosh,³⁵ yielding a frequency of 252 cm^{-1} for the $16b^1$ vibration.

The appearance of symmetry-forbidden vibration with b_2 symmetry may be explained due to vibronic coupling to higher excited states with A_1 symmetry, which calculations are predicted to lie 0.59 eV above the first excited state. Also, for

TABLE 4: Calculated Frequencies and the Isotopic Shifts in the First Excited State (S_1), As Well As the Calculated Frequencies in the Cation Ground State (D_0) (All in cm^{-1})

<i>o</i> DCB					<i>m</i> DCB					<i>p</i> DCB				
mode	symm	S_1		D_0 ν	mode	symm	S_1		D_0 ν	mode	symm	S_1		D_0 ν
		ν	calcd shift				ν	calcd shift				ν	calcd shift	
15	a_1	195	2.8	213	9a	a_1	194	2.1	205	7a	a_g	306	3.8	329
7a	a_1	444	2.4	489	7a	a_1	379	3.8	399	6a	a_g	717	0.9	751
6a	a_1	602	1.3	651	6a	a_1	623	1.0	655	1	a_g	1056	0.8	1093
18b	a_1	915	0.1	995	12	a_1	961	0.0	972	9a	a_g	1174	0.0	1198
1	a_1	1069	0.7	1118	18a	a_1	980	0.0	1099	8a	a_g	1568	0.0	1601
9a	a_1	1159	0.0	1190	1	a_1	1114	0.6	1125	2	a_g	3221	0.0	3153
14	a_1	1719	0.0	1316	19a	a_1	1350	1.0	1419	16a	a_u	260	0.0	360
19a	a_1	1399	0.0	1441	8a	a_1	1553	0.0	1513	17a	a_u	597	0.0	978
8a	a_1	1512	0.0	1523	13	a_1	3190	0.0	3137	10a	b_{1g}	530	0.0	785
20a	a_1	3128	0.0	3205	20a	a_1	3214	0.0	3152	20a	b_{1g}	544	3.6	566
2	a_1	3147	0.0	3217	2	a_1	3227	2.0	3156	12	b_{1u}	948	0.1	981
10a	a_2	76	0.4	93	10a	a_2	139	0.3	165	18a	b_{1u}	1074	0.5	1093
16a	a_2	304	0.1	658	16a	a_2	318	0.1	526	19a	b_{1u}	1453	0.0	1434
4	a_2	457	0.0	658	17a	a_2	610	0.0	911	13	b_{1u}	3206	0.0	3141
17a	a_2	558	0.0	859	10b	b_1	113	0.3	138	10b	b_{2g}	220	0.3	239
5	a_2	662	0.0	991	16b	b_1	282	0.1	371	4	b_{2g}	484	0.0	674
10b	b_1	148	0.1	214	4	b_1	454	0.0	584	5	b_{2g}	619	0.0	961
16b	b_1	277	0.2	425	11	b_1	538	0.0	769	15	b_{2u}	220	1.6	230
11	b_1	520	0.0	763	17b	b_1	533	0.0	869	18b	b_{2u}	1004	0.0	1120
17b	b_1	609	0.0	975	5	b_1	647	0.0	975	14	b_{2u}	1763	0.0	1299
9b	b_2	313	2.8	312	15	b_2	360	1.8	365	15	b_{2u}	1328	0.0	1456
7b	b_2	403	1.4	410	7b	b_2	398	1.6	379	7b	b_{2u}	3216	0.0	3151
6b	b_2	708	1.5	736	6b	b_2	764	1.8	801	9b	b_{3g}	346	0.9	355
12	b_2	980	0.2	1059	18b	b_2	1000	0.3	1030	6b	b_{3g}	572	0.1	579
18a	b_2	1047	0.2	1402	9b	b_2	1179	0.0	1130	3	b_{3g}	530	0.0	1261
3	b_2	1217	0.0	1203	3	b_2	1305	0.0	1265	8b	b_{3g}	1541	0.0	1407
19b	b_2	1389	0.0	1402	14	b_2	1764	0.0	1349	20b	b_{3g}	3206	0.0	3141
8b	b_2	1529	0.0	1514	8b	b_2	1437	0.0	1418	11	b_{3u}	75	0.6	81
13	b_2	3115	0.0	3196	19b	b_2	1562	0.0	1451	16b	b_{3u}	337	0.0	484
20b	b_2	3142	0.0	3215	20b	b_2	3208	0.0	3144	17b	b_{3u}	540	0.1	829

TABLE 5: Observed Vibrational Modes of *o*DCB of the S_1 State Together with Their Symmetries, the Measured Shifts of the $^{35}\text{Cl}_2$ and $^{35}\text{Cl}^{37}\text{Cl}$ Isotopomers, and the Calculated Shifts of the Vibrations (All in cm^{-1})

assignment		symm	ν	measd shift	calcd shift	rel int (exptl)
Wilson	Herzberg					
0^0	0^0	a_1	0	0.0	0.0	100
$10b^1$	20^1	b_1	149	0.0	0.1	13
15^1	11^1	a_1	197	2.2	2.8	4
$16b^1$	19^1	b_1	233	0.0	0.2	9
$9b^1$	30^1	b_2	309	2.7	2.8	38
$7b^1$	29^1	b_2	404	1.3	1.4	9
$7a^1$	10^1	a_1	437	2.4	2.4	90
			560	0.0		5
			580	0.0		7
$6a^1$	9^1	a_1	610	1.4	1.3	34
$16b^17b^1$	19^129^1	a_2	640	0.3	0.2	14
$6b^1$	28^1	b_2	718	1.4	1.5	8
$6a^19b^1$	9^130^1	b_2	919	2.8	4.1	11
			940	0.0	0.0	20
$18b^1$	8^1	a_1	954	0.0	0.0	30
$9b^16b^1$	30^128^1	a_1	1025	4.2	4.3	13
$7a^16a^1$	10^19^1	a_1	1048	4.1	3.8	18
			1058	0.0		7
$16a^27a^1$	15^210^1	a^1	1079	2.8	2.7	13
1^1	7^1	a_1	1088	1.2	0.7	94
			1094	1.6		14
			1106	0.0		8

m-difluorobenzene³⁶ the appearance of vibrations with b_2 symmetry was explained by a benzene-like HT coupling. Symmetry-forbidden bands with b_1 and a_2 symmetry were only observed as the first overtones. Such an observation was also made for *o*- and *m*-difluorobenzenes.³⁴

(c) *p*DCB. The molecule belongs in contrast to the two other isomers to the point group D_{2h} as it has an inversion center. The electronic excitation $S_1 \leftarrow S_0$ is characterized as a $^1B_{2u} \leftarrow ^1A_g$ transition.

The origin of the first excited state is observed at 35 752 cm^{-1} , which is in perfect agreement with the measured value of 35 752 cm^{-1} by Shimoda,¹⁶ as well as the one measured by Anno et al.¹⁵ of 35 750 cm^{-1} . It is a little bit different from the measured value of 35 746 cm^{-1} by Rohlffing et al.¹⁸ and Sands et al.¹⁹ The deviation from the value of 35 731 cm^{-1} obtained by Weickardt et al.¹⁷ can again be explained by their use of vacuum wavelength for laser calibration instead of air wavelength as done in this work.

TABLE 6: Observed Vibrational Modes of *m*DCB of the S_1 State Together with Their Symmetries, the Measured Shifts of the $^{35}\text{Cl}_2$ and $^{35}\text{Cl}^{37}\text{Cl}$ Isotopomers, and the Calculated Shifts of the Vibrations (All in cm^{-1})

assignment		symm	ν	measd shift	calcd shift	rel int (exptl)
Wilson	Herzberg					
0^0	0^0	a_1	0	0.0	0.0	100
$9a^1$	11^1	a_1	201	1.3	2.1	5
$10a^2$	14^2	a_1	270	0.3	0.5	5
$7a^1$	10^1	a_1	365	3.3	3.8	41
15^1	30^1	b_2	378	1.9	1.8	44
$7b^1$	29^1	b_2	390	0.6	1.6	2
$16b^2$	19^2	a_1	504	0.0	0.2	5
$7a^1 9a^1$	$10^1 11^1$	a_1	565	4.2	3.3	5
$15^1 9a^1$	$30^1 11^1$	b_2	575	1.9	1.6	5
$6a^1$	9^1	a_1	607	1.1	1.0	7
$16a^2$	13^2	a_1	680	0.0	0.2	5
$6b^1$	28^1	b_2	762	0.8	1.8	7
12^1	8^1	a_1	961	0.0	0.0	244
$7a^1 6a^1$	$10^1 9^1$	a_1	975	4.1	4.4	44
$15^1 6a^1$	$29^1 9^1$	b_2	986	5.0	4.0	17
$18a^1$	7^1	a_1	1090	0.0	0.0	22
1^1	6^1	a_1	1103	0.7	0.6	78
$9b^1$	26^1	b_2	1124	0.0	0.0	7
			1140	1.4		5
			1159	1.4		5

TABLE 7: Observed Vibrational Modes of *p*DCB of the S_1 State Together with Their Symmetries, the Measured Shifts of the $^{35}\text{Cl}_2$ and $^{35}\text{Cl}^{37}\text{Cl}$ Isotopomers, and the Calculated Shifts of the Vibrations (All in cm^{-1})

assignment		symm	ν	measd shift	calcd shift	rel int (exptl)
Wilson	Herzberg					
0^0	0^0	a_g	0	0.0	0.0	100
11^2	30^2	a_g	150	1.2	1.1	3
$7a^1$	6^1	a_g	298	3.3	3.8	15
$16a^2$	8^2	a_g	332	0.0	0.0	19
$9b^1$	27^1	b_{3g}	337	0.8	0.9	34
$10b^2$	17	a_g	451	0.6	0.6	2
$6b^1$	26^1	b_{3g}	536	0.0	0.1	34
$16b^2$	29^2	a_g	585	0.0	0.2	3
$7a^1 9b^1$	$6^1 27^1$	b_{3g}	638	4.0	4.1	5
$16a^2 9b^1$	$8^2 27^1$	b_{3g}	670	0.7	0.9	3
$6a^1$	5^1	a_g	726	0.7	0.9	78
$7a^1 6b^1$	$6^1 26^1$	b_{3g}	836	3.8	3.3	4
$7a^1 6a^1$	$5^1 6^1$	a_g	1028	4.5	4.0	6
1^1	4^1	a_g	1054	1.1	0.8	18
$9b^1 6a^1$	$27^1 5^1$	b_{3g}	1065	2.4	1.8	36
$20a^2$	14^2	a_g	1093	5.5	7.0	35
$9a^1$	3^1	a_g	1139	0.1	0.0	6

Assignment of the Vibrations. Most of the vibrations in the first excited state are already assigned by Rohlfling et al.¹⁸ and Sands et al.¹⁹ We assist their performed assignment by comparing the measured and calculated frequencies and shifts.

Additionally, the peaks at 451 cm^{-1} [0.0 cm^{-1}] and 1139 cm^{-1} [0.1 cm^{-1}] were assigned as the vibrations $10b^2$ and $9a^1$. The calculated frequencies for these vibrations are 440 cm^{-1} [0.6 cm^{-1}] and 1174 cm^{-1} [0.0 cm^{-1}].

The observation of the nontotally symmetric vibrations with b_{3g} symmetry could be explained due to a coupling to a higher electronic state with B_{1u} symmetry. The same kind of coupling was observed for *p*-difluorobenzene³⁷ and explained by a benzene-like HT coupling. Calculations predict that the symmetry of the second excited state is B_{1u} at an energy of 0.56 eV from the first excited state.

2. MATI Spectra. To gain further insight into these molecular systems, MATI spectra via the 0^0 and the $7a^1$ intermediate states of the three isomers and additionally for *p*DCB via the $6a$ intermediate state were measured. These spectra are displayed in Figures 4–6. For all three isomers the $^{35}\text{Cl}_2$ and the $^{35}\text{Cl}^{37}\text{Cl}$ isotopomers were recorded. The assignment of the vibrational levels in the D_0 state is performed by comparing the experimental and calculated frequencies (Tables 4 and 8–10).

(a) *o*DCB. Ionization Energy. The main feature in the MATI spectrum via the electronic origin of the first excited state of the two investigated isotopomers (Figure 4a,b) is the observance of the 0^0 transition with overwhelming intensity. This behavior is due to the well-known propensity rule^{38,39} ($\Delta\nu = 0$). The origin of the ${}^2B_1(D_0)$ state and therewith the adiabatic ionization energy is determined to be $73\,237 \pm 6 \text{ cm}^{-1}$ ($9.0799 \pm 0.0006 \text{ eV}$). It is worth mentioning that this is the most precise value measured until now. There are several values published in the literature^{40–44} varying from 9.06 to 9.24 eV. From these values the one obtained by Watanabe et al.¹³ in 1962 of $9.07 \pm 0.01 \text{ eV}$ is the one that corresponded best with our measured value. They performed photoelectron spectroscopy, but their results of the other two isomers differ significantly from the values of our measurements.

Assignment of the Vibrations. The peaks appearing at 210, 489, and 653 cm^{-1} were assigned as the total symmetric vibrations 15^1 , $7a^1$, and $6a^1$ because the measured frequencies are in great accordance with the calculated ones of 213, 489, and 653 cm^{-1} . Also, the $7b^1$ mode with b_2 symmetry is detected at 408 cm^{-1} , which is calculated to 410 cm^{-1} .

Notable Features of the Spectra. The MATI spectrum via the $7a^1$ mode, displayed in Figure 4c, shows great similarity to the

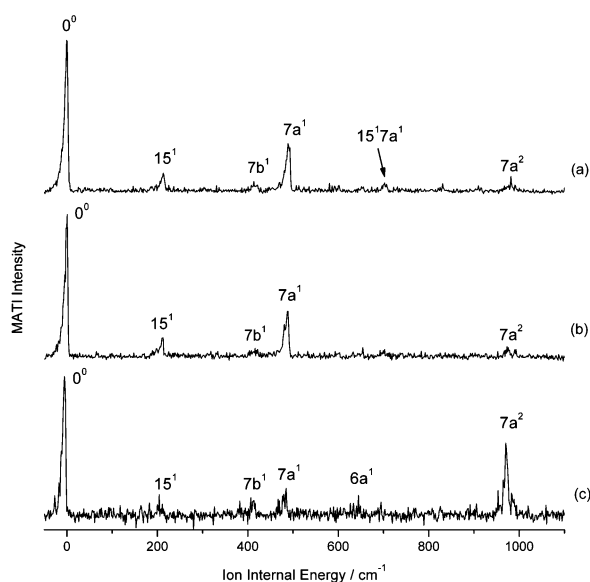


Figure 4. MATI spectra of *o*DCB via the electronic origin of the S_1 state of (a) the $^{35}\text{Cl}_2$ isotopomer and (b) the $^{35}\text{Cl}^{37}\text{Cl}$ isotopomer. In (c) the recorded MATI spectrum via the $7a^1$ mode of *o*DCB is shown.

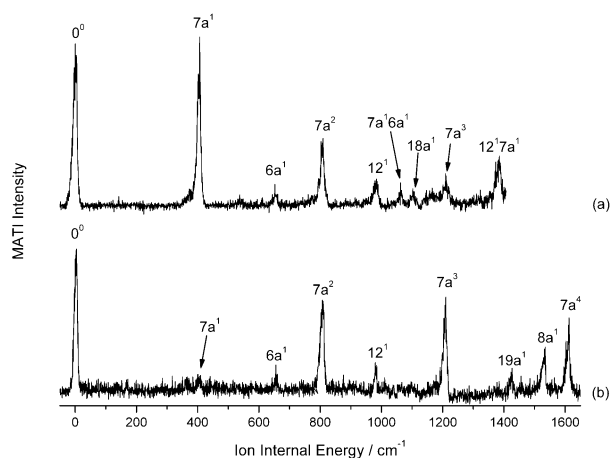


Figure 5. MATI spectra via (a) the lowest intermediate state and (b) the $7a^1$ mode of *m*DCB.

spectrum via the lowest intermediate state observing the electronic origin as the strongest peak. However, the intensities of the $7a^1$ (at 489 cm^{-1}) and $7a^2$ (980 cm^{-1}) modes are exchanged compared to the MATI spectrum via the origin of the S_1 state. As a result, the propensity rule is not fulfilled, indicating a geometry change at the transition from the excited state to the ion ground state, which will be discussed in detail below.

(b) *m*DCB. Ionization Energy. For *m*DCB the resulting MATI spectrum via the origin of the S_1 state is shown in Figure 5a. The origin of the ionic ground state and therewith the adiabatic ionization energy is determined to be $73\,776 \pm 6\text{ cm}^{-1}$ ($9.1471 \pm 0.0008\text{ eV}$). This value is the most precise value until now. Former measurements yielded values between 9.28^{43} and 9.10 eV^{40} .

Assignment of the Vibrations. The peaks appearing at 403 , 653 , 981 , 1107 , 1425 , and 1535 cm^{-1} were assigned as the vibrations $7a^1$, $6a^1$, 12^1 , $18a^1$, $19a^1$, and $8a^1$ because the measured frequencies fit very well with the calculated ones of 399 , 655 , 972 , 1099 , 1419 , and 1513 cm^{-1} , respectively.

Notable Features of the Spectra. In the spectrum via the origin of the first electronically excited state, the propensity rule is not fulfilled. The vertical transition into the ionic origin is

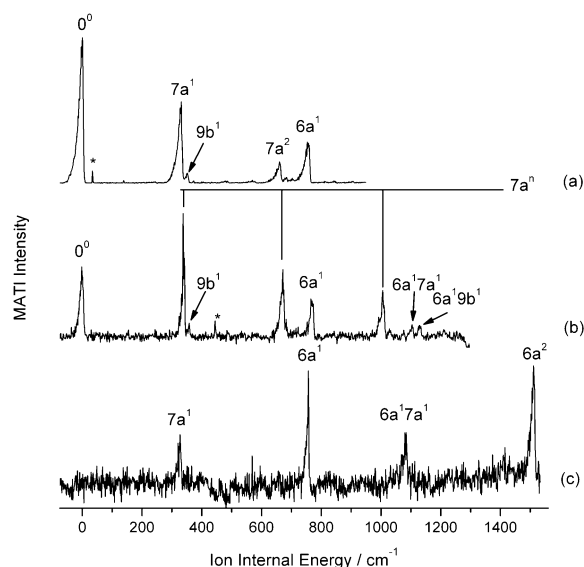


Figure 6. MATI spectra of *p*DCB (a) via the electronic origin, (b) via the $7a^1$ mode, and (c) via the $6a^1$ mode in the first excited state.

observed with the same intensity as the $7a^1$ mode. Moreover, this spectrum is dominated by the $7a^1$ mode and its overtones.

In the spectrum via the $7a^1$ vibration (Figure 5b) of the S_1 state, the propensity rule is also not fulfilled. The $7a^1$ mode is observed very weakly, while the progression bands $7a^2$ to $7a^4$ and the electronic origin dominate the spectrum.

(c) *p*DCB. Ionization Energy. Figure 6a shows the resulting MATI spectra via the vibrationless intermediate electronic state. As seen, the propensity rule is fulfilled. The origin of the D_0 state and accordingly the adiabatic ionization energy of both isotopomers of *p*DCB is determined to be $72\,191 \pm 6\text{ cm}^{-1}$ ($8.9506 \pm 0.0007\text{ eV}$). Former measurements yielded values of 8.92 ± 0.03 , 40 8.95 , 43 and $8.97 \pm 0.03\text{ eV}^{41}$.

Assignment of the Vibrations. The peaks appearing at 334 and 758 cm^{-1} were assigned as the total symmetric vibrations $7a^1$ and $6a^1$ because the measured frequencies correspond very well with the measured ones of 399 and 655 cm^{-1} . We assigned the peak at 354 cm^{-1} as the $9b^1$ mode having b_{3g} symmetry which is in good accordance with the calculated frequency of 355 cm^{-1} .

Notable Features of this Spectrum. In the MATI spectrum via the origin of the first excited state, the $7a$ and $6a$ vibrations are observed with high intensity. In the MATI spectrum via the $7a^1$ mode (Figure 6b) the vertical transition is the prominent peak and the spectrum is dominated by a progression of the $7a$ mode. The MATI spectrum via the $6a^1$ mode in the S_1 state (Figure 6c) shows two peaks with the same intensity which are assigned as the $6a^1$ mode and its first overtone, which is observed with a remarkably high intensity. Such a strong appearance of the first overtone of the $6a$ vibration was also observed for *p*-fluorotoluene. 46

Discussion

1. Effect of Halogen Substitution on Transition Energy.

Table 11 lists the origins of the $S_1 \leftarrow S_0$ transition and the adiabatic ionization energies for halogen-substituted molecules including dichlorobenzenes, difluorobenzenes, fluorophenols, and fluoroanilines. A halogen atom such as chlorine or fluorine can interact with the aromatic ring by the inductive effect through the σ bond and by the mesomeric effect through the π orbitals. The inductive effect depends on the electronegativity of the halogen atom. Therefore, it is greater for fluorine than

TABLE 8: Observed and Calculated Frequencies (cm⁻¹) for the Electronic Ground State (S₀), the First Electronically Excited State (S₁), and the Ion Ground State (D₀) of *o*DCB

mode		S ₀			S ₁			D ₀	
Wilson	Herzberg	symm	exptl ^a	DFT (C _{2v})	exptl	CASSCF ^b (C _s)	CIS ^b (C _{2v})	exptl	DFT ^c (C _{2v})
15	11	a ₁	203	202	197	195	203	210	213
7a	10	a ₁	480	477	437	444	445	489	489
6a	9	a ₁	660	671	610	602	619	653	651
18b	8	a ₁	1041	1056	954	915	995		995
1	7	a ₁	1130	1139	1088	1069	1125		1118
9b	30	b ₂	334	338	309	313	314		312
7b	29	b ₂	429	427	404	403	407	408	410
6b	28	b ₂	740	746	718	708	726		736
10b	20	b ₁	241	233	149	148	101		214
16b	19	b ₁	435	449	233	277	276		425

^a Taken from ref 25. ^b Calculated values are scaled by a scaling factor of 0.95. ^c Calculated values are scaled by a scaling factor of 0.98.

TABLE 9: Observed and Calculated Frequencies (cm⁻¹) for the Ground State (S₀), the First Excited State (S₁), and the Ion Ground State (D₀) of *m*DCB^a

mode		S ₀			S ₁			D ₀	
Wilson	Herzberg	symm	exptl ^b	DFT (C _{2v})	exptl	CASSCF ^c (C _s)	CIS ^c (C _{2v})	exptl	DFT ^d (C _{2v})
9a	11	a ₁	198	197	201	194	201		205
7a	10	a ₁	399	397	365	379	379	403	399
6a	9	a ₁	663	674	607	623	631	653	655
12	8	a ₁	999	1012	961	961	1002	981	972
18a	7	a ₁	1068	1094	1090	980	1070	1107	1099
19a	5	a ₁	1124	1129	1103	1114	1156	1145	1125
8a	4	a ₁	1576	1612		1553	1421	1535	1513
<i>10b</i>	<i>14</i>	<i>a</i> ₂	<i>212</i>	<i>201</i>	<i>135</i>	<i>139</i>	<i>149</i>		<i>165</i>
<i>16a</i>	<i>13</i>	<i>a</i> ₂	<i>531</i>	<i>551</i>			<i>368</i>		<i>538</i>
<i>16b</i>	<i>19</i>	<i>b</i> ₁	<i>428</i>	<i>445</i>	<i>252</i>	<i>282</i>	<i>236</i>		<i>371</i>
15	30	b ₂	366	369	379	360	373		365
7b	29	b ₂	430	431	390	398	393		379
6b	28	b ₂	784	783	763	764	798		801

^a Vibrations that were only observed as overtones are given in italics. ^b Taken from ref 25. ^c Calculated values are scaled by a scaling factor of 0.95. ^d Calculated values are scaled by a scaling factor of 0.98.

TABLE 10: Observed and Calculated Frequencies (cm⁻¹) for the Ground State (S₀), the First Excited State (S₁), and the Ion Ground State (D₀) of *p*DCB^a

mode		S ₀			S ₁			D ₀	
Wilson	Herzberg	symm	exptl	DFT	exptl	CASSCF	CIS	exptl	DFT
7a	6	a _g	328	328	298	306	308	334	329
6a	5	a _g	747	754	726	717	753	758	751
1	4	a _g	1096	1099	1054	1056	1109		1093
<i>16a</i>	<i>8</i>	<i>a</i> _u	<i>410</i>	<i>420</i>	<i>166</i>	<i>260</i>	<i>40</i>		<i>360</i>
<i>11</i>	<i>30</i>	<i>b</i> _{3u}	<i>125</i>	<i>101</i>	<i>75</i>	<i>75</i>	<i>83</i>		<i>81</i>
<i>16b</i>	<i>29</i>	<i>b</i> _{3u}	<i>485</i>	<i>500</i>	<i>293</i>	<i>337</i>	<i>434</i>		<i>484</i>
9b	27	b _{3g}	350	358	337	346	356	354	355
6b	26	b _{3g}	626	640	536	572	562		579

^a Vibrations that were only observed as overtones are given in italics.

for chlorine. The mesomeric effect reflects the overlap of the π system and the halogen, which is greater for the larger and more polarizable chlorine atom. The respective electronic excitation energies for the ortho, meta, and para isomers of dichlorobenzene are smaller than for the monosubstituted chlorobenzene. They are red shifted by 810, 851, and 1328 cm⁻¹, respectively. The observed red shift in the excitation energies suggests that the interaction between the chlorine atoms and the aromatic ring is stronger in the upper electronic state than in the lower one.

The electronic excitation of benzene derivatives corresponds to a $\pi^* \leftarrow \pi$ transition, leading to an expansion of the aromatic ring. This fits with the results of our theoretical calculations. The chlorine atoms can stabilize the system by the mesomeric effect. In contrast, *o*-difluorobenzene and *m*-difluorobenzene, where the electron-withdrawing inductive effect is more distinctive, show a slight blue shift compared to the monosubstituted fluorobenzene molecule. Only the electronic excitation energy of *p*-difluorobenzene is slightly red shifted as an effect of the

collective results. This is the case for fluorophenols and fluoroanilines as well. It is notable that the red shift for the para isomers of the two latter substances is in the magnitude of the shift of *p*DCB, which underlines the dependence of stabilization of the substituents' relative positions.

The theoretical calculations show that the D₀ ← S₀ transition corresponds to the removal of an electron of a π orbital. This causes a shortening of the C–Cl bond and of the central C–C bond of the ring. For chlorobenzene the geometry changes during ionization to a more quinoid structure³ as the positive charge in the aromatic ring is to some extent quenched by the donation from a lone-pair electron from the chlorine.

For the adiabatic ionization energy one finds that they follow the order para < ortho < meta. This seems to be a general trend for halogen-substituted aromatic compounds. In comparison to chlorobenzene, the ionization energy of *p*DCB is red shifted by about 980 cm⁻¹. The notable decrease indicates the great stabilization of the *p*DCB cation where the chlorine atoms

TABLE 11: Electronic Transition and Ionization Energies (cm⁻¹) of Chlorobenzene, Dichlorobenzenes, Fluorobenzene, and Difluorobenzenes, As Well As Phenol, Aniline, and Their *o*-, *m*-, and *p*-Fluoro-Substituted Derivatives Determined by REMPI, Fluorescence Excitation, MATI, and ZEKE Experiments

	$S_1 \leftarrow S_0$	ΔE_1	IE	ΔE	ref
chlorobenzene	37 048		73 170		3
<i>o</i> DCB	36 238	-810	73 237	67	this work
<i>m</i> DCB	36 193	-851	73 776	606	this work
<i>p</i> DCB	35 752	-1328	72 191	-979	this work
fluorobenzene	37 819		74 238		2
<i>o</i> -difluorobenzene	37 824	5	75 003	765	5, 6
<i>m</i> -difluorobenzene	37 909	90	75 332	1094	5, 6
<i>p</i> -difluorobenzene	36 840	-979	73 861	-377	5, 6
phenol	36 349		68 625		
<i>o</i> -fluorophenol	36 804	455	70 006	1381	7, 47
<i>m</i> -fluorophenol, <i>cis</i>	36 623	274	70 188	1563	8
<i>m</i> -fluorophenol, <i>trans</i>	36 829	480	70 449	1824	8
<i>p</i> -fluorophenol	35 117	-1232	68 577	-48	9
aniline	34 029		62 271		12, 48
<i>o</i> -fluoroaniline	34 583	554	63 644	1373	10
<i>m</i> -fluoroaniline	34 614	585	64 159	1888	11
<i>p</i> -fluoroaniline	32 652	-1377	62 543	272	12

stabilize the positive charge of the aromatic ring by the mesomeric effect. The ionization energy of *o*DCB is higher than that of *p*DCB but is nearly the same as that of chlorobenzene, which indicates that the mesomeric stabilization and the steric interaction of the two chlorine atoms are nearly compensating each other. For *o*DCB and *p*DCB the geometry changes during ionization to a more quinoid structure, whereas *m*DCB cannot be stabilized in the same way because of the relative positions of the chlorine atoms at the aromatic ring. The weaker stabilization of the positive charge in the *m*DCB cation explains the higher ionization energy compared to the ortho isomer, though their excitation energies into the S_1 state are nearly the same.

All three isomers show a greater relative stabilization than the respective isomers of the fluorobenzene derivatives. Thus, in the case of the para isomer the red shift of the dichlorobenzene is larger than for difluorobenzene, fluorophenol, and fluoroaniline.

2. Isotope Effect on the Transition Energies. For chlorobenzene Lembach and Brutschy³⁹ recorded MATI spectra via different intermediate states for the ³⁵Cl and ³⁷Cl isotopomers. They found that no isotopic shift occurs either for the $S_1 \leftarrow S_0$ excitation energy or for the ionization energy. Their results are in coincidence with the results presented here for the ³⁵Cl₂ and the ³⁷Cl³⁵Cl isotopomers of the dichlorobenzenes, where also no shift could be observed.

3. Effect of the Chlorine Position and of the Substitution of Isotopes on Molecular Vibration. The performed calculations of the three isomers show that the frequencies of two vibrational modes in benzene in the region around 3000 cm⁻¹ are dramatically decreased to around 300–500 cm⁻¹ in dichlorobenzene. The appearance of the two former C–H-stretching modes is notably changed due to the substitution with two heavy chlorine atoms. One of these modes in all three dichlorobenzenes is the 7a vibration. One can expect to observe an isotopic effect in this normal vibration because of the significant participation of the chlorine atoms in this mode. We experimentally determined the isotopic shift, yielding 2.4 cm⁻¹ for the ortho isomer and 3.3 cm⁻¹ for the meta and para isomers in the first electronically excited state.

Further, the measured and calculated frequencies in the S_1 state are slightly lower than in the S_0 state and in the D_0 state. This indicates that the molecular geometry in the S_1 state is not as rigid as in the S_0 and D_0 states, which is supported by the calculated geometries and the assumption that the electronic excitation corresponds to a $\pi^* \leftarrow \pi$ transition.

4. Geometry Change upon $D_0 \leftarrow S_1$ Excitation. The calculations predict a strong geometry change along the 7a vibration for all three isomers. The appearance of such a geometry change would also explain several features of the observed MATI spectra. For *o*DCB the breakdown of the propensity rule in the MATI spectrum via the 7a vibration would be in coincidence with such a geometry change. Also, the breakdown of the propensity rule in the MATI spectra via the origin and the 7a vibration of the first excited state of *m*DCB would be explained, as well as the observation of overtones and combination bands involving the 7a vibration. In the case of *p*DCB this geometry change would be responsible for the appearance of overtones and progressions involving the 7a vibration.

Because the propensity rule is fulfilled for the MATI spectra of *p*DCB, while for *o*DCB a breakdown in the MATI spectrum via the 7a mode is observed and for *m*DCB the propensity rule is fulfilled neither in the MATI spectrum via the origin nor via the 7a mode, it is concluded that the strength of the geometry change follows the order *p*DCB < *o*DCB < *m*DCB. This deviates from the theoretical results, which suggest the order to be *o*DCB < *m*DCB < *p*DCB. Obviously, the calculation of the overlap between the projected atomic displacement vector and the eigenvector of the modes gives only a hint for the appearing progressions in the MATI spectra.

In the case of *p*DCB an additional breakdown of the propensity rule occurs by ionization via the 6a¹ intermediate state. This feature is attributed to a geometry change along the 6a mode upon ionization, as is also shown by the performed calculations. Therefore the 6a¹ vibration is also detected in the MATI spectrum via the electronic origin of the S_1 state with great intensity. A similar observation was made for chlorobenzene^{2,45} and *p*-fluorotoluene,⁴⁶ where the 6a¹ vibration was observed with great intensity in the spectrum via the origin of the S_1 state. Besides, for the latter molecule a breakdown of the propensity rule was detected by excitation via the overtone of the 6a vibration as well. These observations were interpreted to occur due to a geometry change along the 6a mode.

Conclusion

We have applied REMPI and MATI techniques to record vibrationally resolved spectra of the first electronically excited state and the cation ground state of the ³⁵Cl₂ and ³⁵Cl³⁷Cl isotopomers of the three isomers of dichlorobenzene. Analyzing the MATI spectra via the lowest intermediate state gives the adiabatic ionization energies with an uncertainty of 6 cm⁻¹. The

results of the experimental studies show no shift for the ionization energy of the different chlorine isotopomers. The ionization energies of the three isomers of dichlorobenzene follow the order para < ortho < meta. With the results reported in the literature this seems to be a general trend for halogen-substituted benzene derivatives. The more polarizable chlorine atoms stabilize the cation state better than fluorine atoms. Thus, the ionization energies are influenced by the relative position and by the nature of the substituents.

As shown, in the S₁ state the substitution of a second chlorine atom effects a red shift of the excitation energy for all three isomers compared to chlorobenzene due to a stronger mesomeric stabilization.

References and Notes

- (1) Imhof, P.; Kleinermanns, K. *Chem. Phys.* **2001**, *270*, 227.
- (2) Walter, K.; Scherm, K.; Boesl, U. *J. Phys. Chem.* **1991**, *95*, 1188.
- (3) Wright, T. G.; Panov, S. I.; Miller, T. A. *J. Chem. Phys.* **1995**, *102*, 4793.
- (4) Reiser, G.; Rieger, D.; Wright, T. G.; Mueller-Dethlefs, K.; Schlag, E. W. *J. Phys. Chem.* **1993**, *97*, 4335.
- (5) Kwon, C. H.; Kim, H. L.; Kim, M. S. *J. Chem. Phys.* **2003**, *118*, 6327.
- (6) Tsuchiya, Y.; Takazawa, K.; Fujii, M.; Ito, M. *J. Phys. Chem.* **1992**, *96*, 99.
- (7) Yuan, L.; Li, C.; Lin, J.; Yang, S.; Tzeng, W. *Chem. Phys.* **2006**, *323*, 429.
- (8) Yosida, K.; Suzuki, K.; Ichiuchi, S.; Sakai, M.; Fujii, M.; Dessent, M.; Mueller-Dethlefs, K. *Phys. Chem. Chem. Phys.* **2002**, *4*, 2534.
- (9) Zhang, B.; Li, C.; Su, H.; Lin, L.; Tzeng, W. B. *Chem. Phys. Lett.* **2004**, *390*, 65.
- (10) Lin, J.; Tzeng, W. B. *Chem. Phys. Phys. Chem.* **2000**, *2*, 3759.
- (11) Lin, J.; Lin, K.; Tzeng, W. *Appl. Spectrosc.* **2001**, *55*, 120.
- (12) Lin, J. L.; Lin, K. C.; Tzeng, W. B. *J. Phys. Chem. A* **2002**, *106*, 6462.
- (13) Mueller-Dethlefs, K.; Sander, M.; Schlag, E. W. *Chem. Phys. Lett.* **1984**, *112*, 291.
- (14) Zhu, L.; Johnson, P. M. *J. Chem. Phys.* **1991**, *94*, 5769.
- (15) Anno, T.; Matubara, I. *J. Chem. Phys.* **1955**, *23*, 796.
- (16) Shimoda, A.; Hikida, T.; Mori, Y. *J. Phys. Chem.* **1979**, *83*, 1309.
- (17) Weickhardt, C.; Zimmermann, R.; Schramm, K. W.; Boesl, U.; Schlag, E. W. *Rapid Commun. Mass Spectrom.* **1994**, *8*, 381.
- (18) Rohlfling, E. A.; Rohlfling, C. M. *J. Phys. Chem.* **1994**, *93*, 94.
- (19) Sands, W. D.; Moore, R. *J. Phys. Chem.* **1989**, *93*, 101.
- (20) Szczepanski, J.; Personette, W.; Pellow, R.; Chandrasekhar, T. M.; Roser, D.; Cory, M.; Zerner, M.; Vala, M. *J. Chem. Phys.* **1992**, *92*, 35.
- (21) Gunzer, F.; Grotemeyer, J. *Phys. Chem. Chem. Phys.* **2002**, *4*, 5966.
- (22) Gunzer, F.; Grotemeyer, J. *Int. J. Mass Spectrom.* **2003**, *228*, 921.
- (23) Frisch, M. J.; Trucks, G. W.; Schlegel, H. B.; Scuseria, G. E.; Robb, M. A.; Cheeseman, J. R.; Montgomery, J. A., Jr.; Vreven, T.; Kudin, K. N.; Burant, J. C.; Millam, J. M.; Iyengar, S. S.; Tomasi, J.; Barone, V.; Mennucci, B.; Cossi, M.; Scalmani, G.; Rega, N.; Petersson, G. A.; Nakatsuji, H.; Hada, M.; Ehara, M.; Toyota, K.; Fukuda, R.; Hasegawa, J.; Ishida, M.; Nakajima, T.; Honda, Y.; Kitao, O.; Nakai, H.; Klene, M.; Li, X.; Knox, J. E.; Hratchian, H. P.; Cross, J. B.; Adamo, C.; Jaramillo, J.; Gomperts, R.; Stratmann, R. E.; Yazyev, O.; Austin, A. J.; Cammi, R.; Pomelli, C.; Ochterski, J. W.; Ayala, P. Y.; Morokuma, K.; Voth, G. A.; Salvador, P.; Dannenberg, J. J.; Zakrzewski, V. G.; Dapprich, S.; Daniels, A. D.; Strain, M. C.; Farkas, O.; Malick, D. K.; Rabuck, A. D.; Raghavachari, K.; Foresman, J. B.; Ortiz, J. V.; Cui, Q.; Baboul, A. G.; Clifford, S.; Cioslowski, J.; Stefanov, B. B.; Liu, G.; Liashenko, A.; Piskorz, P.; Komaromi, I.; Martin, R. L.; Fox, D. J.; Keith, T.; Al-Laham, M. A.; Peng, C. Y.; Nanayakkara, A.; Challacombe, M.; Gill, P. M. W.; Johnson, B.; Chen, W.; Wong, M. W.; Gonzalez, C.; Pople, J. A. *Gaussian 03*, revision A.1; Gaussian, Inc.: Pittsburgh, PA, 2003.
- (24) Becke, A. D. *J. Chem. Phys.* **1993**, *98*, 56.
- (25) Scheerer, J. R.; Evans, J. E. *Spectrochim. Acta* **1962**, *19*, 1739.
- (26) Wilson, E. B. *Phys. Rev.* **1934**, *45*, 706.
- (27) Lord, R. C.; Marston, A. L.; Miller, F. A. *Spectrochim. Acta* **1957**, *9*, 113.
- (28) Herzberg, G. *Molecular Spectra and Molecular Structure II: Infrared and Raman Spectra of Polyatomic Molecules*; Van Nostrand: New York, 1945.
- (29) Mulliken, R. S. *J. Chem. Phys.* **1955**, *23*, 1997.
- (30) Foresman, B.; Gordon, M. H.; Pople, J. A.; Frisch, M. J. *J. Phys. Chem.* **1992**, *96*, 135.
- (31) Potts, A. W.; Lyus, M. L.; Lee, E. P. F.; Fattahallah, G. H. *J. Chem. Soc., Faraday Trans. 2* **1980**, *76*, 556.
- (32) Kwon, C. H.; Kim, H. L.; Kim, M. S. *J. Chem. Phys.* **2003**, *118*, 6327.
- (33) Swinn, A. K.; Kable, S. H. *J. Mol. Spectrosc.* **1998**, *191*, 49.
- (34) Tsuchiya, Y.; Takazawa, K.; Fujii, M.; Ito, M. *Chem. Phys. Lett.* **1991**, *183*, 107.
- (35) Meenakshi, A.; Ghosh, D. K. *J. Mol. Spectrosc.* **1984**, *103*, 195.
- (36) Graham, P. A.; Kable, S. H. *J. Chem. Phys.* **1995**, *103*, 6426.
- (37) Knight, A. E. W.; Kable, S. C. *J. Chem. Phys.* **1988**, *89*, 7139.
- (38) Mueller-Dethlefs, K.; Schlag, E. W. *Angew. Chem., Int. Ed.* **1998**, *37*, 1346.
- (39) Lembach, G.; Brutschy, B. *J. Chem. Phys.* **1997**, *107*, 6156.
- (40) Olesik, S.; Baer, T.; Morrow, J. C. *J. Phys. Chem.* **1986**, *90*, 3563.
- (41) Ruscic, B.; Klasinc, L.; Wolf, A.; Knop, J. V. *J. Phys. Chem.* **1981**, *85*, 1486.
- (42) Watanabe, K.; Nakayama, T.; Mottl, J. J. *Quant. Spectrosc. Radiat. Transfer* **1962**, *2*, 369.
- (43) Fujisawa, S.; Oonishi, I.; Masuda, S.; Ohno, K.; Harada, Y. *J. Phys. Chem.* **1991**, *95*, 4250.
- (44) Kimura, K.; Katsumata, S.; Achiba, Y.; Yamazaki, T.; Iwata, S. *Handbook of HeI Photoelectron Spectra of Fundamental Organic Compounds*; Japan Scientific Society Press: Tokyo, 1981.
- (45) Ripoche, X.; Dimicoli, I.; Le Calve, J.; Piuze, F.; Botter, R. *Chem. Phys.* **1988**, *124*, 305.
- (46) Ayles, V. L.; Hammond, C. J.; Bergeron, D. E.; Richards, O. J.; Wright, T. G. *J. Chem. Phys.* **2007**, *126*, 244304.
- (47) Dopfer, O.; Müller-Dethlefs, K. *J. Chem. Phys.* **1994**, *101*, 8508.
- (48) Takahashi, M.; Ozeki, H.; Kimura, K. *J. Chem. Phys.* **1992**, *96*, 6399.